The 4th Joint International Conference on Multibody System Dynamics
May 29 – June 2, 2016, Montréal, Canada

Dynamic modelling of a four-bar free floating mechanism with passive joints and flywheel actuators

David St-Onge[1] and Clément Gosselin[2]

[1]*Department of Mechanical Engineering, Université Laval, Québec, Qc, Canada, david.st-onge.2@ulaval.ca*
[2]*Department of Mechanical Engineering, Université Laval, Québec, Qc, Canada, gosselin@gmc.ulaval.ca*

ABSTRACT — *This paper introduces a novel actuation approach for a free-floating four-bar planar mechanism. In the proposed arrangement, which is mainly geared towards space applications, the configuration and orientation of the mechanism is controlled by flywheels mounted on each of the links, while the joints connecting the links are passive. The dynamic model of the system is derived using Kane's equations, adapted for a closed-chain multibody system. Simulation results are presented to confirm the approach. The stability of the resolution of the equations is then investigated using the condition number of the generalized inertia matrix and the impact of the geometric parameters on this stability is studied.*

1 Introduction

Four-bar and five-bar mechanisms are commonly used in robotics and in machines. Replacing the links of serial robots by four-bar or five-bar mechanisms increases the stiffness, which can be a great advantage for large payloads [1]. Robots based on planar five-bar linkages, which are sometimes referred to as a dual-arm SCARA, are available for industrial or educational applications (see for instance Fig.1). Compared to a serial drive mechanism, a parallelogram five-bar mechanism has large structural stiffness and low moving inertia [2]. In fact, most mechanisms can have one or many of their links replaced with a parallelogram to improve their stiffness, as it was shown for some parallel robots in [3]. Nevertheless, the Type 1 singularities of the open chains remain and new Type 2 singularities emerge in such robotic architectures. For instance, a parallelogram collapsing onto a line constitutes such an uncertain configuration [4], or Type 2 singularity. The approach presented here is able to overcome this kind of singularity using actuation redundancy.[5]

The four-bar mechanism discussed in this paper is being developed as an exploratory concept to study the potential of a novel actuation strategy for deployable mechanisms in space applications [6]. Previous research has pointed out the complexity of controlling the deployment of a space structure with minimal impact on the base satellite [7, 8]. The four current most popular solutions consist in generating impulse torques from thrusters, in order to spin the entire spacecraft or to use reaction wheels or moment gyroscopes [9]. For a spacecraft manipulators, the wheels and gyroscopes, when positioned on the arm links were shown to be more energy efficient than thrusters [10]. Specifically for four-bar mechanisms, a solution involving couterweights was proposed in [11], but the added mass is counterproductive, especially for space applications.

Fig. 1: DexTAR robot from Mecademic.

This paper first presents the derivation of the dynamic equations of a planar four-bar mechanism without any actuators at the joints but rather with flywheels mounted on each of the links. Based on the matrix equations obtained, simulations are performed

and the results are compared to those obtained from a commercial multibody simulation software. The last section of the paper analyses the equations in order to assess the influence of the different design parameters on the conditioning of the general inertia matrix of the system.

2 Dynamic equations

Since deployable mechanisms based on rigid links can be made of closed kinematic chains, this study explores the potential of using flywheels mounted on the links of a planar four-bar mechanism to provide an effective actuation scheme. According to the Chebyshev-Grübler-Kutzbach criterion and since the mechanism studied is planar and not grounded, each joint constrains two of the planar degrees of mobility, yielding

$$l = 3n - 2j = 4, \tag{1}$$

where l is the degree of freedom, n is the number of links and j the number of joints. Since four flywheels are used, the mechanism is redundantly actuated with respect to the two controllable degrees of freedom, namely the orientation of one of the links and the configuration of the four-bar mechanism. Indeed, although the mechanism has four degrees of freedom, two of these degrees of freedom correspond to the translational motion of the centre of mass of the mechanism, which cannot be controlled by the actuators. Hence, two flywheels would be sufficient to control the attitude and configuration of the mechanism. The advantage of using four flywheels is that it provides control redundancy and it allows one to make all the links identical. The variables chosen to describe the configuration of the mechanism are the position of the centre of mass of the first link (x_A,y_A), and the orientation of each of the four links given by ϕ_A, ϕ_B, ϕ_C and ϕ_D which are defined with respect to a fixed frame (**i**, **j**) as shown in Fig.2. The motion equations are derived using Kane's approach in which $\mathbf{R}_i$ is defined as the rotation matrix from body i to the inertial frame. The generalized independent velocities (noted u_i, i=1,...,4) are chosen to be the two velocity components of the centre of mass of one of the links and the angular velocities of two of the four links with respect to the inertial frame. It follows that the velocity of the centre of mass of each of the links and the angular velocity of the links can be written in terms of the generalized velocities as:

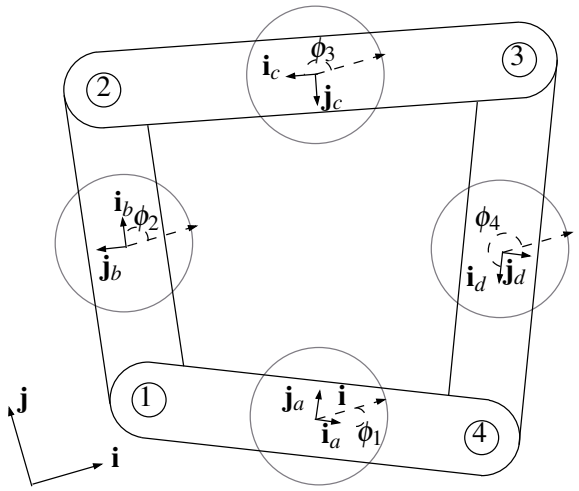

Fig. 2: Schematic representation of the four-bar mechanism with each body reference frame and their flywheel.

$$\begin{aligned}
\mathbf{v}_A &= u_1\mathbf{i} + u_2\mathbf{j},\ \omega_A = u_3\mathbf{k},\ \omega_B = u_4\mathbf{k} \\
\mathbf{v}_B &= \mathbf{v}_A + \omega_A\mathbf{E}\mathbf{r}^{A1} - \omega_B\mathbf{E}\mathbf{r}^{B1} = u_1\mathbf{i} + u_2\mathbf{j} + u_3\mathbf{E}\mathbf{r}^{A1} - u_4\mathbf{E}\mathbf{r}^{B1} \\
\mathbf{v}_C &= \mathbf{v}_B + \omega_B\mathbf{E}\mathbf{r}^{B2} - \omega_C\mathbf{E}\mathbf{r}^{C2} \\
\mathbf{v}_D &= \mathbf{v}_C + \omega_C\mathbf{E}\mathbf{r}^{C3} - \omega_D\mathbf{E}\mathbf{r}^{D3},
\end{aligned}$$

with

$$\mathbf{E} = \begin{bmatrix} 0 & -1 \\ 1 & 0 \end{bmatrix}, \tag{2}$$

the matrix coefficient equivalent to a cross product of a vector in the i,j plane with k, and where **i**, **j** and **k** are the unit vectors defining the inertial frame, where **k** is orthogonal to the plane of motion, where $\mathbf{r}^{ui}$ is the position vector of joint i with respect to the centre of mass of link u expressed in the inertial frame. It should be noted that the constraint induced by joints 1,2 and 3 are included in the definition of the velocities $\mathbf{v}_B$,$\mathbf{v}_C$ and $\mathbf{v}_D$, but not the closure constraint of the mechanism. In order to eliminate the dependent unknowns ω_C and ω_D, the loop closure constraint is written as:

$$\mathbf{r}_{12} + \mathbf{r}_{23} = \mathbf{r}_{14} + \mathbf{r}_{43}, \tag{3}$$

which can be written as:

$$\mathbf{R}_B\mathbf{r}_{12}^B + \mathbf{R}_C\mathbf{r}_{23}^C = \mathbf{R}_A\mathbf{r}_{14}^A + \mathbf{R}_D\mathbf{r}_{43}^D, \tag{4}$$

where r_{ij}^k are the constant vector from a joint to the next in the body reference frame of link k. Differentiating the above equation with respect to time then yields

$$\begin{aligned}
\mathbf{E}\mathbf{R}_B\omega_B\mathbf{r}_{12}^B + \mathbf{E}\mathbf{R}_C\omega_C\mathbf{r}_{23}^C &= \mathbf{E}\mathbf{R}_A\omega_A\mathbf{r}_{14}^A + \mathbf{E}\mathbf{R}_D\omega_D\mathbf{r}_{43}^D \\
\begin{bmatrix}\mathbf{R}_A\mathbf{r}_{14}^A & -\mathbf{R}_B\mathbf{r}_{12}^B\end{bmatrix}\begin{Bmatrix}\omega_A\\ \omega_B\end{Bmatrix} &= \begin{bmatrix}\mathbf{R}_C\mathbf{r}_{34}^C & -\mathbf{R}_D\mathbf{r}_{43}^D\end{bmatrix}\begin{Bmatrix}\omega_C\\ \omega_D\end{Bmatrix},
\end{aligned}$$

The angular velocity of bodies c and d can therefore be expressed as a linear combination of two of the generalized independent velocities:

$$\begin{aligned}
\omega_C &= \gamma_1 u_3 + \gamma_2 u_4 \\
\omega_D &= \gamma_3 u_3 + \gamma_4 u_4.
\end{aligned}$$

and $\mathbf{v}_C$ and $\mathbf{v}_D$ then become:

$$\begin{aligned}
\mathbf{v}_C &= u_1\mathbf{i} + u_2\mathbf{j} + u_3\mathbf{E}\mathbf{r}^{A1} - u_4\mathbf{E}\mathbf{r}^{B1} + u_4\mathbf{E}\mathbf{r}^{B2} - (\gamma_1 u_3 + \gamma_2 u_4)\mathbf{E}\mathbf{r}^{C2} \\
\mathbf{v}_D &= u_1\mathbf{i} + u_2\mathbf{j} + u_3\mathbf{E}\mathbf{r}^{A1} - u_4\mathbf{E}\mathbf{r}^{B1} + u_4\mathbf{E}\mathbf{r}^{B2} - (\gamma_1 u_3 + \gamma_2 u_4)\mathbf{E}\mathbf{r}^{C2} + (\gamma_1 u_3 + \gamma_2 u_4)\mathbf{E}\mathbf{r}^{C3} - (\gamma_2 u_3 + \gamma_4 u_4)\mathbf{E}\mathbf{r}^{D3}.
\end{aligned}$$

The above equations are readily differentiated in order to obtain the expressions for the accelerations of points A, B, C and D, noted $\mathbf{a}_A$ to $\mathbf{a}_D$, which are then used to build the expressions of the virtual forces F_i^*as

$$\begin{aligned}
F_i^* &= \frac{\partial \mathbf{v}_A}{\partial u_i}\cdot(-\mathbf{a}_A m_A) + \frac{\partial \mathbf{v}_B}{\partial u_i}\cdot(-\mathbf{a}_B m_B) + \frac{\partial \omega_A}{\partial u_i}\cdot(-\alpha_A I_A) + \frac{\partial \omega_B}{\partial u_i}\cdot(-\alpha_B I_B) \\
&\quad + \frac{\partial \mathbf{v}_C}{\partial u_i}\cdot(-\mathbf{a}_C m_C) + \frac{\partial \mathbf{v}_D}{\partial u_i}\cdot(-\mathbf{a}_D m_D) + \frac{\partial \omega_C}{\partial u_i}\cdot(-\alpha_C I_C) + \frac{\partial \omega_D}{\partial u_i}\cdot(-\alpha_D I_D) \\
F_1^* &= -m_T\dot{u}_1,\ F_2^* = -m_T\dot{u}_2 \\
F_3^* &= (\mathbf{E}\mathbf{r}_{A1})(-m_b\mathbf{a}_b) - I_a\alpha_a + (\mathbf{E}\mathbf{r}_{A1} - \gamma_1\mathbf{E}\mathbf{r}_{C2})(-m_C\mathbf{a}_c) \\
&\quad - I_C\alpha_C + (\mathbf{E}\mathbf{r}_{A1} - \gamma_1\mathbf{E}\mathbf{r}_{C2} + \gamma_1\mathbf{E}\mathbf{r}_{C3} - \gamma_3\mathbf{E}\mathbf{r}_{D3})(-m_D\mathbf{a}_D) - \gamma_3 I_D\alpha_D \\
F_4^* &= (-\mathbf{E}\mathbf{r}_{B1})(-m_b\mathbf{a}_b) - I_b\alpha_b + (-\mathbf{E}\mathbf{r}_{B1} + \mathbf{E}\mathbf{r}_{B2} - \gamma_2\mathbf{E}\mathbf{r}_{C2})(-m_C\mathbf{a}_c) \\
&\quad - \gamma_2 I_C\alpha_C + (-\mathbf{E}\mathbf{r}_{B1} + \mathbf{k}\times\mathbf{r}_{B2} - \gamma_2\mathbf{E}\mathbf{r}_{C2} + \gamma_2\mathbf{E}\mathbf{r}_{C3} - \gamma_4\mathbf{E}\mathbf{r}_{D3})(-m_D\mathbf{a}_D) - \gamma_4 I_D\alpha_D,
\end{aligned}$$

where $\alpha_i = \dot{\omega}_i$.

The external forces $F_i, i = 1,\ldots,4$, of the flywheels are similarly developed from:

$$F_i = \frac{\partial \omega_{fA}}{\partial u_i}\cdot(\dot{\omega}_{fA}I_{fA}) + \frac{\partial \omega_{fB}}{\partial u_i}\cdot(\dot{\omega}_{fB}I_{fB}) + \frac{\partial \omega_{fC}}{\partial u_i}\cdot(\dot{\omega}_{fC}I_{fC}) + \frac{\partial \omega_{fD}}{\partial u_i}\cdot(\dot{\omega}_{fD}I_{fD}), \tag{5}$$

which leads to $F_1 = F_2 = 0$, $F_3 = I_{fA}\dot{\omega}_{fA} + \gamma_1 I_{fC}\dot{\omega}_{fC} + \gamma_3 I_{fD}\dot{\omega}_{fD}$ and $F_4 = I_{fB}\dot{\omega}_{fB} + \gamma_2 I_{fC}\dot{\omega}_{fC} + \gamma_4 I_{fD}\dot{\omega}_{fD}$, where fu is the flywheel on body u and $\dot{\omega}_{fu}$ its angular acceleration.

The resulting matrix system can be written as

$$\begin{bmatrix}
-m_T & 0 & A_1(\phi_1) & B_1(\phi_2) & C_1(\phi_3) & D_1(\phi_4) \\
0 & -m_T & A_2(\phi_1) & B_2(\phi_2) & C_2(\phi_3) & D_2(\phi_4) \\
A_3(\phi_1) & B_3(\phi_1) & C_3(\phi_2) & D_3(\phi_1,\phi_2) & E_3(\phi_1,\phi_3) & F_3(\phi_1,\phi_4) \\
A_4(\phi_3) & B_4(\phi_3) & C_4(\phi_1,\phi_3) & D_4(\phi_2,\phi_3) & E_4(\phi_3) & F_4(\phi_3,\phi_4)
\end{bmatrix}\begin{Bmatrix}\dot{u}_1\\ \dot{u}_2\\ \dot{u}_3\\ \dot{u}_4\end{Bmatrix} + \begin{Bmatrix}
E_1(\phi_1,\phi_2,\phi_3,\phi_4,u_3^2,u_4^2,u_5^2,u_6^2) \\
E_2(\phi_1,\phi_2,\phi_3,\phi_4,u_3^2,u_4^2,u_5^2,u_6^2) \\
G_3(\phi_1,\phi_2,\phi_3,\phi_4,u_3^2,u_4^2,u_5^2,u_6^2) \\
G_4(\phi_1,\phi_2,\phi_3,\phi_4,u_3^2,u_4^2,u_5^2,u_6^2)
\end{Bmatrix}$$
$$= \begin{bmatrix}
0 & 0 & 0 & 0 \\
0 & 0 & 0 & 0 \\
-I_{fA} & 0 & -\gamma_1 I_{fC} & -\gamma_2 I_{fD} \\
0 & -I_{f2} & -\gamma_2 I_{fC} & -\gamma_4 I_{fD}
\end{bmatrix}\begin{Bmatrix}\dot{\omega}_{f1}\\ \dot{\omega}_{f2}\\ \dot{\omega}_{f3}\\ \dot{\omega}_{f4}\end{Bmatrix},$$

which is simplified by removing the translational accelerations of link 1. Indeed, the first two equations are independent from the input forces , which is consistent with the fact that the acceleration of the centre of mass of the system cannot be controlled. The first two equations are then readily solved for $\dot{u}_1$ and $\dot{u}_2$, which are then substituted into the other equations in order to obtain a reduced system that can be written as

$$\mathbf{A}_{2\times2}\dot{\mathbf{u}}_{2\times1} + \mathbf{b}_{2\times1} = \mathbf{I}_{f,2\times4}\dot{\boldsymbol{\omega}}_{f,4\times1} \tag{6}$$

For a given desired trajectory, the above equations can be used to determine the required flywheel accelerations. This reduced formulation highlights the redundancy of the mechanism. Four actuated flywheels allow to control two degrees of freedom. For many applications, such as space structures, redundancy is mandatory to ensure a system robust to failures. In this case, mounting a flywheel on each link also simplifies the manufacturing and modelling steps by standardizing the links.

3 Simulation results

In order to validate the dynamic model derived above, SolidWorks and SimMechanics are used. The SimMechanics model of the links includes a single flywheel and a planar constraint to the fixed frame to ensure that the movement remains in the plane. In parallel, simulations are performed using the matrix form of the equations with the same inputs.

In order to simulate a simplified system, all the links are taken as identical, with $m_i = 0.02kg$, $I_i = 2.2 \times 10^{-5} kg.m^2$, $I_{f,u} = 3.4 \times 10^{-7} kg.m^2$ and a length of $0.1m$. Two different tests were performed in an open-loop mode. First, two opposite flywheels on links a and c were actuated with an angular position following a cosine function for 10 seconds. The results shown in Fig.3-a demonstrate that the absolute orientation of links 2 and 4 (b and d) follows the periodic function while the orientation of the other two remains constant. The second test involves all four flywheels rotating following the same command. Fig.3-b shows that the whole mechanism rotates as if it were a rigid body, thus conserving the same configuration. In the same way, actuating two opposite flywheels with opposite commands does not produce any change in the configuration or orientation of the mechanism. These special case inputs produce intuitively expected movements that are suitable to validate the models.

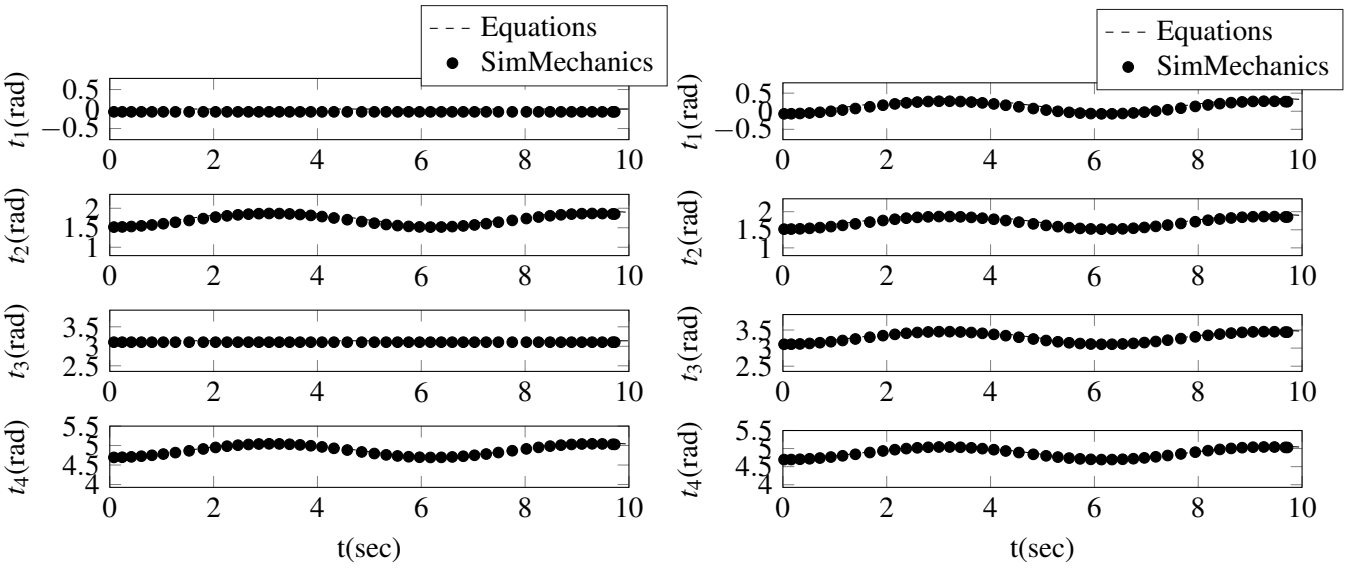

Fig. 3: Comparison of the results obtained using the dynamic model based on Kane's equations and with SimMechanics for cosine inputs: a- on the angular position of 2 flywheels mounted on opposite links on a four-bar, four-flywheel mechanism, b- on all flywheels.

The results obtained with the above formulation based on Kane's equations match the simulation results with slight differences. The root mean square error for the first test is 0.100 while for the second test it is 0.102. The two

links of the first test whose orientation should remain constant are rotating a little due to some inaccuracies in the 3D CAD model that was used to develop the SimMechanics model, thus decreasing the amplitude of the movement on the other two. For the second test, a similar behaviour tends to induce a small change in the mechanism configuration (difference between consecutive links orientation). Further study of the behaviour of the equations with respect to the geometric parameters of the mechanism will clarify these differences.

4 Optimization of the energy consumption using redundancy

Eq. 6 shows that the mechanical system has two controllable degrees of freedom, which supports Eq. 1 since the translation of the centre of mass of the system, which cannot be controlled, was removed from the derivation. The application targeted by this mechanism consists of large space structures with hundreds of similar closed kinematic chains. Therefore, the manufacturing and assembly process were simplified from the beginning by assuming similar properties and actuation means for each of the links. Thus, the mechanism has four flywheels — four actuator inputs — for two controllable degrees of freedom, i.e., two outputs, which leads to actuation redundancy and an overdetermined system of equations. The simulations of the previous section used predetermined input functions, equal for each pair of opposite flywheels. In fact, for these simple maneuvers the solutions used above minimize the energy consumption of the actuators. For instance, if only one flywheel was used to create the movement of Fig. 3-a the required energy would be larger.

Energy is difficult to obtain in space, either by long-term harvesting of solar power or from chemicals brought in the spacecraft payload. The main concern of each motorized system is then to minimize its energy consumption. Considering that each flywheel has the same inertia, it follows that the optimal solution for a desired trajectory of the mechanism should minimize the instantaneous kinetic energy

$$E = \sum_{i=1}^{4} \frac{\mathbf{I}_{fi}}{2} \omega_{fi}^2, \tag{7}$$

while satisfying the constraint from Eq. 6.

Using Lagrange multipliers and differentiating the relation with respect to each of the unknowns, the solution to minimize the norm of the flywheel accelerations is

$$\dot{\omega}_f = -\mathbf{I_f}^T (\mathbf{I_f} \mathbf{I_f}^T)^{-1} (\mathbf{A}\dot{\mathbf{u}} - \mathbf{b}), \tag{8}$$

From this relation the inputs required to change the orientation of links a and d following a soft step (step of $\frac{\pi}{2}$ with both derivatives equal to zero at the start and at the end) were computed and compared to the same trajectory using only the minimum required to actuate the system, its two flywheels. Fig. 4 shows the instantaneous total kinetic energy of the flywheels and the cumulative ideal power required to actuate the flywheels,

$$P(t) = P(t-1) + \sum_{i=1}^{4} I_{fi} \left| \dot{\omega}_{fi}(t)(\theta_{fi}(t) - \theta_{fi}(t-1)) \right|. \tag{9}$$

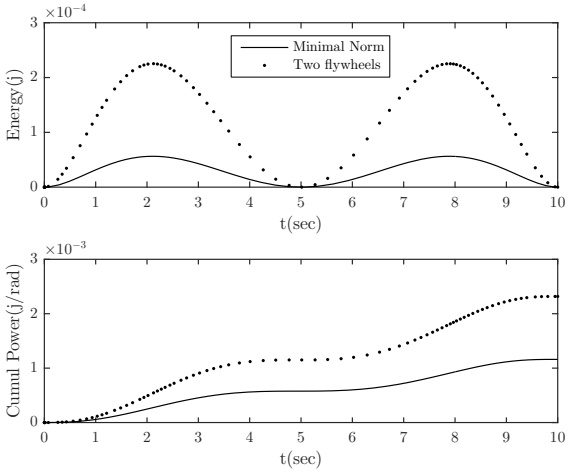

Fig. 4: Comparison of the energy required for a soft-step trajectory by minimizing the norm of the acceleration or using only 2 of the 4 flywheels.

These results show that the more flywheels the system has, the better the performances will be, since the peak velocity of each flywheel will be less. On the other hand, this conclusion only depends on the inertia of the flywheel, i.e., the bigger the total inertia of the flywheels, the smaller their velocities will be. Obviously increasing the weight of the actuators is not beneficial for space applications. This is why the previous derivation used constant flywheel inertia (1/10th of the link

inertia) and aim to create a trajectory known to be reachable for such configurations within 10s. Larger movement amplitude can always be achieved with more delay, which is not considered problematic in space where time is more available than energy.

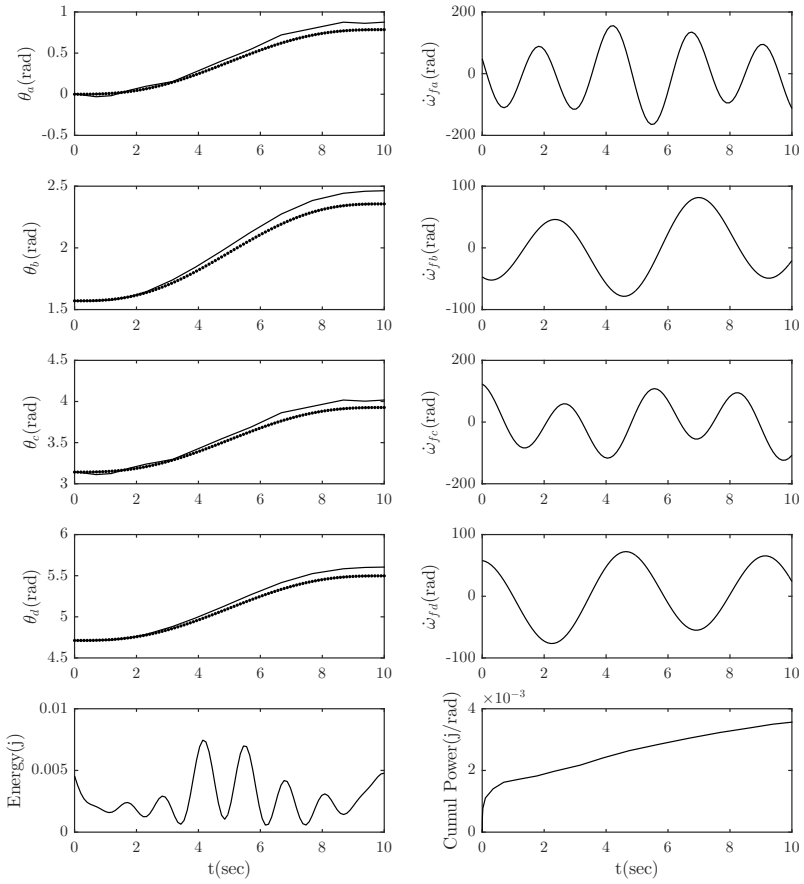

Fig. 5: Result of an optimisation with genetic algorithm of the flywheel trajectories and inertias to minimize the power for a soft-step trajectory of the whole mechanism.

The previous approach minimizes the instantaneous kinetic energy of the system, but a better representation of the actuator's consumption is the cumulative output power required, which is not necessarily minimized by this approach. Since the derivation of a Lagrange multiplier relation to minimize the power lead to a complex set of differential equations to be solved simultaneously, a forward unconstrained optimization process was preferred to validate the results. Fig.5 shows the result using the CMA-ES (Covariance Matrix Adaptation Evolution Strategy) optimization [12] to minimize the mean square error over the whole trajectory while simultaneously trying to minimize the cumulative power required to complete the trajectory. If small errors are allowed, it is shown that non identical flywheels ($I_{f1} = 0.88I_{f0}$,$I_{f2} = 0.41I_{f0}$,$I_{f3} = 1.37I_{f0}$ and $I_{f4} = 0.77I_{f0}$) following different trajectories is one optimal output of the run, but perform similarly.

5 Influence of the geometric parameters

The results presented in Section 3 demonstrated that the mathematical model obtained using Kane's equations yields correct results. This model can then be used to assess the behaviour of the system as a function of the geometric parameters of the mechanism. Several metrics were defined in the literature for a four-bar mechanism, a review of them was presented in [5]. In the context of this study, the condition number of matrix $\mathbf{A}$ is first observed.

It is well known that if the condition number of matrix $\mathbf{A}$ remains close to 1, the stability of the equations is ensured. The mechanism is free-floating and its behaviour is not expected to change with its global position or orientation. On the other hand, its configuration may impact the performance of the actuators. Both studies of Fig.6 show the evolution of the condition number over a wide range of the angle between link a and link b, representing the configuration of the four-bar. The condition number of matrix $\mathbf{A}_{2,2}$ is presented in Fig.6-a as a function of the ratio of the length of link a to link b. For this study, a parallelogram shape is assumed ($l_c = l_a$ and $l_d = l_b$). The

effect of this ratio is independent from the mechanism configuration ($\theta_1 = \phi_b - \phi_a$, from Fig.2) and tends to bias the condition number when above or under 1. The second test involves the offset of the mass centre of each link from the line connecting neighbouring joints (y coordinate in body frame). All links were offset similarly for this study. For configurations corresponding to small internal angles between link a and b the offset of link a and c toward the centre keeps the condition number stable for a larger span of offset values than in the opposite direction of the mechanism configuration.

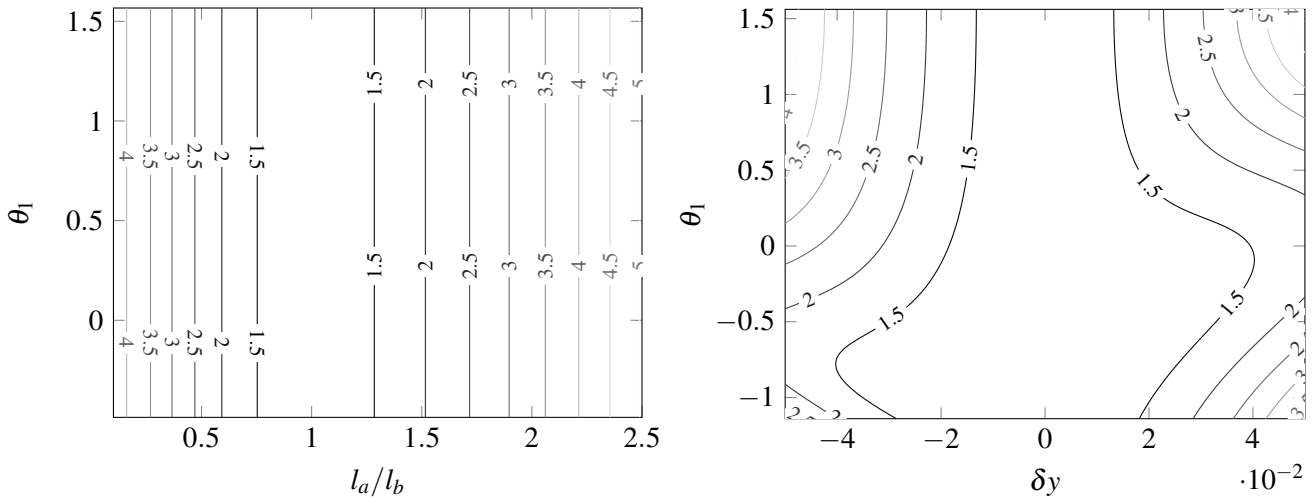

Fig. 6: Influence of the (a) the length of link a to the length of link b ratio (b) the offset position of the mass centre of all links on the condition number.

Generally, for four-bar mechanisms actuated by their joints, the singularity of collapsed links leads to a configuration in which the output joint of the four-bar mechanism is free to move even if the input joint is locked. In [1] a solution for a five-bar mechanism is proposed by either separating the input joint in 2 joints or by changing the geometry of one of the links so that it has the same mass as the other but is shorter. In this case shortening two face-to-face links increases the condition number (see Fig.6-a), but is not required since no singularity arise in the $\theta_1 = 0$ configuration.

6 Conclusions

A free-floating planar four-bar mechanism whose attitude and configuration are controlled using flywheels mounted on the links was presented in this paper. The equations of motion were derived using Kane's formulation and a dynamic model was obtained. The model was validated by comparing the results with those obtained with SimMechanics for specific input motions. The singularities and sensitivity of the mathematical representation and the physics of the mechanism were discussed. It was observed that the symmetry of the link geometry yields a more stable kinematic arrangement. A prototype is to be built and tested on a free-floating frictionless table to validate the results of this paper.

Acknowledgements

The authors would like to acknowledge the financial support of the Natural Sciences and Engineering Research Council of Canada (NSERC) and the Canada Research Chair Program.

References

[1] D. N. NENCHEV and M. UCHIYAMA, "Para-arm: A five-bar parallel manipulator with singularity-perturbed design," *Mechanism and Machine Theory*, vol. 33, pp. 453–462, 1998.

[2] J. Kim, "Task based kinematic design of a two dof manipulator with a parallelogram five-bar link mechanism," *Mechatronics*, vol. 16, pp. 323–329, 2006.

[3] X.-J. Liu and J. Wang, "Some new parallel mechanisms containing the planar four-bar parallelogram," *International Journal of Robotics Research*, vol. 22(9), pp. 717–732, 2003.

[4] K.-L. Ting, "Gross motion and classification of manipulators with closed-loop, four-bar chains," *International Journal of Robotics Research*, vol. 11(3), pp. 238–247, 1992.

[5] V. Mermertas, "Optimal design of manipulator with four-bar mechanism," *Mechanism and Machine Theory*, vol. 39, pp. 545–554, 2004.

[6] D. St-Onge and C. Gosselin, "Deployable mechanisms for small to medium-sized space debris removal," in *Proceedings of the 65th International Astronautical Congress*, Sept. 29 – Oct. 3,Toronto, Canada 2014.

[7] M. K. Kwak, S. Heo, and H. B. Kim, "Dynamics of satellite with deployable rigid solar arrays," *Multibody Systems Dynamics*, vol. 20, pp. 271–286, 2008.

[8] S. Dubowsky and E. Papdopoulos, "The kinematics, dynamics, and control of free-flying and free-floating space robotic systems.," *IEEE Tansactions on robotics and automation*, vol. 9, pp. 531–543, 1993.

[9] P. C. Hughes, *Spacecraft attitude dynamics*. Courrier Corporation, 2012.

[10] M. Carpenter, *Dynamics and control of gyroscopically actuated space-robotic systems*. Cornell University Press, PhD thesis, 2009.

[11] Q. Jiang and C. Gosselin, "Dynamic optimization of reactionless four-bar linkages," *Journal of Dynamic Systems, Measurement, and Control*, vol. 132 (4), p. 041006, 2010.

[12] S. Kern, S. Müller, N. Hansen, D. Büche, J. Ocenasek, and P. Koumoutsakos, "Learning probability distributions in continuous evolutionary algorithms–a comparative review," *Natural Computing*, vol. 3, no. 1, pp. 77–112, 2004.